

Mossbauer effect study of as-quenched, annealed and crystallised $\text{Fe}_{95-x}\text{W}_5\text{B}_x$ metallic glasses

This article has been downloaded from IOPscience. Please scroll down to see the full text article.

1990 J. Phys.: Condens. Matter 2 4227

(<http://iopscience.iop.org/0953-8984/2/18/019>)

View [the table of contents for this issue](#), or go to the [journal homepage](#) for more

Download details:

IP Address: 171.66.16.96

The article was downloaded on 10/05/2010 at 22:07

Please note that [terms and conditions apply](#).

Mössbauer effect study of as-quenched, annealed and crystallised $\text{Fe}_{95-x}\text{W}_5\text{B}_x$ metallic glasses

K Ganesan, A Narayanasamy and T Nagarajan

Department of Nuclear Physics, University of Madras, Guindy Campus, Madras-600 025, India

Received 6 September 1989

Abstract. A ^{57}Fe Mössbauer effect study of the as-quenched, annealed and crystallised $\text{Fe}_{95-x}\text{W}_5\text{B}_x$ metallic glasses with $x = 15, 20$ and 25 has been performed. For the as-quenched alloys, the fitting of the room-temperature Mössbauer spectra by the Window method yields the most probable and average hyperfine magnetic fields which appear to increase linearly with increasing boron concentration. The opposite trend observed in the variation of Mössbauer hyperfine parameters with temperature of annealing for the $x = 15$ and 25 alloys at high annealing temperatures is due to changes taking place in the dense random packing structure of the alloys at the composition with $x \approx 20$. The Mössbauer studies of the crystallised $\text{Fe}_{80}\text{W}_5\text{B}_{15}$ specimen show that the alloy undergoes a eutectic type of crystallisation. The different crystalline phases that emerge during the crystallisation of the present system are found to be $\alpha\text{-Fe}$, Fe_2B , $(\text{Fe}_{0.8}\text{W}_{0.2})_3\text{B}$ and a non-magnetic FeWB phase.

1. Introduction

The physical properties of Fe–TM–B metallic glasses greatly depend on the nature of the added transition-metal (TM) element. Studies in the literature (Lovas *et al* 1980, Granasy *et al* 1982) show that the introduction of elements such as Mo, W, Nb and Ti into Fe–B metallic glasses improves the magnetic permeability and thermal stability and reduces the AC core loss of the material. Studies on mass density, magnetic after-effect (MAE), magnetic anisotropy, isomer shift, etc, of the Fe–W–B metallic glass system have been reported in the literature (Nielsen 1980, Kisdi-Koszo *et al* 1982, Novak *et al* 1982, Kiss *et al* 1984, Konczos *et al* 1984, Takacs *et al* 1984, Toth *et al* 1985, Sas *et al* 1986). The objectives of the present work are to study the effect of W introduction into the Fe–B metallic glass system on the magnetic hyperfine interactions and to detect the structural changes with boron concentration. The effect of thermal annealing on the Mössbauer hyperfine parameters and the crystallisation behaviour of the Fe–W–B system are also described.

2. Experimental details

The metallic glass ribbons of $\text{Fe}_{95-x}\text{W}_5\text{B}_x$ with $x = 15, 20$ and 25 have been prepared by the single-roller technique (Nielsen 1980). The ribbons are about 1–2 mm wide and have a thickness of 30–40 μm . The amorphicity of the alloys was checked by x-ray diffraction.

Mössbauer effect measurements were made at room temperature (RT) for the alloys in their as-quenched, isochronally and isothermally annealed and crystallised states. To record the Mössbauer spectra of the alloys, absorbers were prepared by placing five to six ribbons each about 15 mm long adjacent and parallel to one another and holding them in position by means of adhesive tape. Annealing and crystallisation of the alloys were carried out as follows. The metallic glass ribbons were put into a thick quartz tube which was then evacuated to a pressure of 10^{-6} Torr and sealed. The sealed tube was inserted into a resistive furnace which was set at the temperature required for annealing or for crystallisation of the alloy, as the case may be. The temperature of annealing was kept within ± 5 K of the desired value. After each such heat treatment, the Mössbauer spectra were recorded at room temperature. For isochronal anneals, a new specimen was used for each temperature. In the case of isothermal annealing, the same pieces of ribbon were heat treated every time and the spectra were recorded at RT after each successive annealing.

3. Results and discussion

3.1. Room-temperature Mössbauer effect study of the as-quenched alloys

Mössbauer spectra were recorded at RT for compositions with $x = 15, 20$ and 25 , in their as-quenched state. The experimental spectra were fitted and deconvoluted to obtain the distribution of the magnetic hyperfine field $P(H)$ by the Window (1971) method. In order to determine the appropriate number m of cosine terms to be used for fitting the present data, the spectrum for the $\text{Fe}_{80}\text{W}_5\text{B}_{15}$ metallic glass at RT has been fitted with various values of m . For the $P(H)$ distributions the values of the average hyperfine field H_{av} have been determined using

$$H_{\text{av}} = \int HP(H) dH / \int P(H) dH.$$

The variations in χ^2 , the most probable magnetic hyperfine field H_p , the full width at half-maximum (FWHM), Γ of the most probable or the most prominent hyperfine field distribution and H_{av} obtained for various values of m are shown in figure 1. All the parameters become constant when m is in the range $12 \leq m \leq 15$. At lower values of m , χ^2 is high and the values of H_p and Γ fluctuate. Similar results have been obtained for other compositions (Ganesan *et al* 1988). Thus, we suggest that the Window method of analysis for the present system is appropriate when $m = 12$ – 15 whereas Chien and Hasegawa (1978) and Chien *et al* (1979) have found $m = 12$ – 20 as the suitable range for the Fe–B metallic glass system. All the spectra shown in this article have been fitted with a value of $m = 15$. The quadrupole interaction was not included in the fitting since, at temperatures $T < T_c$, the angular factor for the effective electric quadrupole interaction is spatially averaged to nearly zero and hence the effective quadrupole interaction is expected to be negligible (Chien *et al* 1979).

Figure 2(a) shows the Mössbauer spectra of the as-quenched $\text{Fe}_{95-x}\text{W}_5\text{B}_x$ alloys at RT. The corresponding $P(H)$ curves are shown in figure 2(b). Oscillations are produced in the $P(H)$ curves at very low and high fields owing to truncations of the Fourier series. As no physical meaning could be attached to them, $P(H)$ distributions are presented in the figures without these oscillations. Chien and Hasegawa (1978) report that the $P(H)$ distribution at RT for the simplest form of Fe–based metallic glass, i.e. for $\text{Fe}_{80}\text{B}_{20}$, is

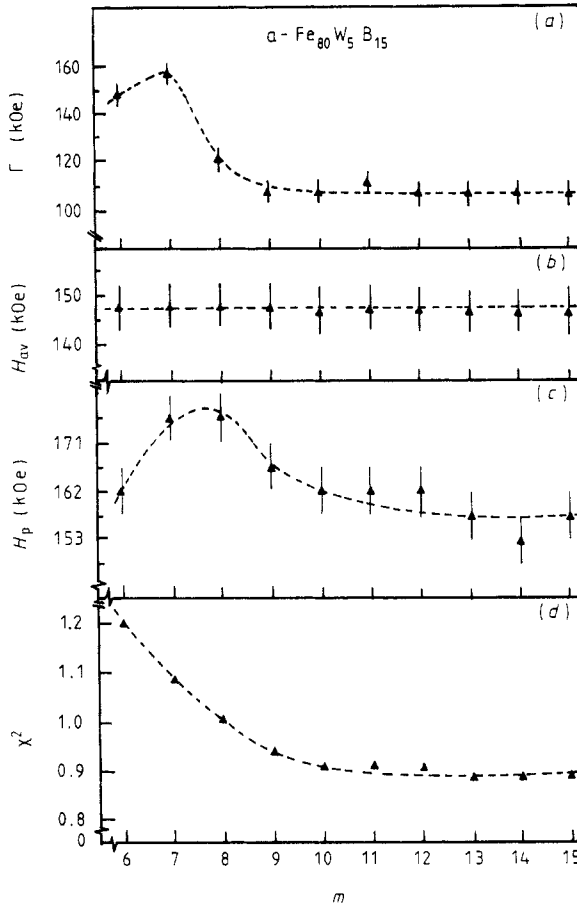


Figure 1. Variations in (a) the FWHM, Γ , (b) the average hyperfine field H_{av} , (c) the peak hyperfine field H_p and (d) χ^2 for various numbers m of cosine terms used in the Window method.

symmetric and single peaked with a value of about 250 kOe for the most probable field and 80 kOe for the FWHM. On replacement of boron by 5 at. % W in the above alloy, i.e. for the $Fe_{80}W_5B_{15}$ metallic glass, we find that the peak field H_p has shifted drastically to a lower value of 157.5 kOe. The decrease in H_p and also that in the value of the saturation magnetic moment at 0 K observed for this alloy (Ramasamy *et al* 1987) may be due to the effect of the relative atomic sizes of Fe and W atoms. The $P(H)$ distribution has become asymmetric with a much broader FWHM of 108 kOe, which is very much higher than that for $Fe_{80}B_{20}$. A value of about 91 kOe for the FWHM has been reported (Bhatnagar and Bhanu Prasad 1985) for $Fe_{67}Co_{18}B_{14}Si_1$. In the case of crystalline disordered binary alloys such as Ni_3Fe and $FeCo$, values of about 41 kOe for the FWHM have been found (Narayanasamy *et al* 1979) and are attributed to the predominant contributions from the first two nearest-neighbour shells of Fe. The higher values of Γ obtained in the present system may be due to interactions extending over significantly longer distances (Bhatnagar and Bhanu Prasad 1985). This argument is further supported by large values of the mean square correlation range of interaction obtained for the present system

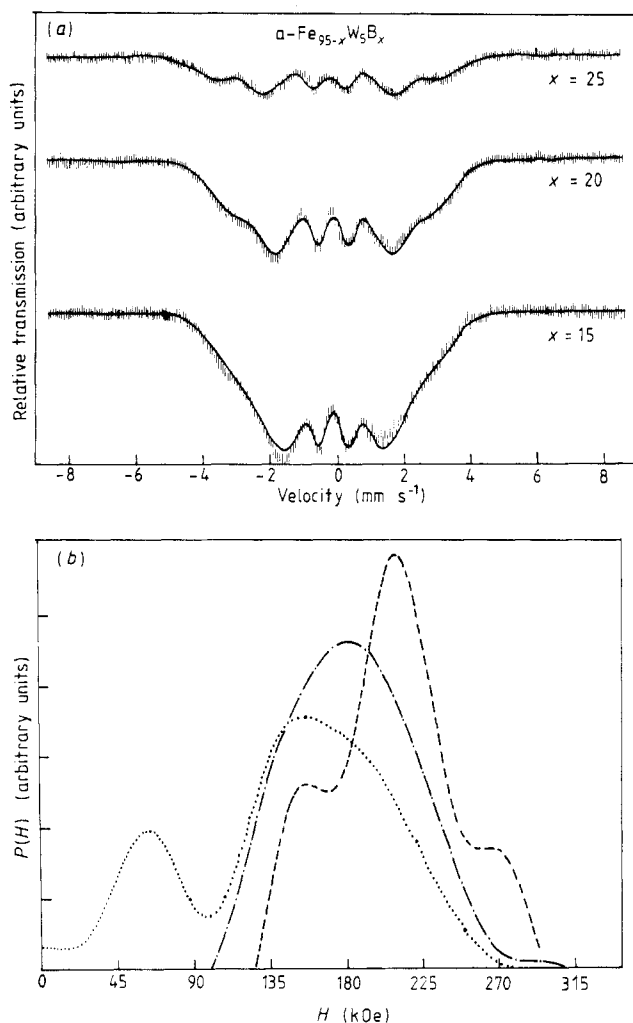


Figure 2. (a) RT Mössbauer spectra. (b) $P(H)$ distribution curves for the as-quenched alloys at RT: \cdots , $x = 15$; $-\cdot-\cdot-$, $x = 20$; $---$, $x = 25$.

(Ramasamy *et al* 1987). The $P(H)$ distribution as such refers to the probable distribution of Fe nearest neighbours and such a large FWHM is related to a high dispersion in the average number of nearest neighbours of Fe atoms. In addition to the above, the $P(H)$ curve for the $x = 15$ alloy has developed a low-field peak at about 53 kOe, which may be due to Fe atoms surrounded by a large number of W atoms. The $x = 25$ alloy exhibits three peaks centred at 157.5, 211.5 and 265.5 kOe in the $P(H)$ distribution, indicating the presence of three different types of Fe environment. Such a multiple-peaked $P(H)$ distribution has also been observed in the case of the $\text{Fe}_{80-x}\text{W}_x\text{B}_{14}\text{Si}_6$ (Lin *et al* 1981) and $\text{Fe}_{40}\text{Ni}_{38}\text{Mo}_4\text{B}_{18}$ (Gopinathan *et al* 1982) metallic glasses. Lin *et al* (1981) present a value of 175 kOe for H_{av} at RT for $\text{Fe}_{75}\text{W}_5\text{B}_{14}\text{Si}_6$ whereas a value of 183 kOe has been obtained for the $\text{Fe}_{75}\text{W}_5\text{B}_{20}$ alloy in the present study.

The variations in H_p , H_{av} and Γ with boron concentration in the present system are shown in figure 3. The variations in Γ_L and Γ_R are also presented in the figure. Γ_L is the

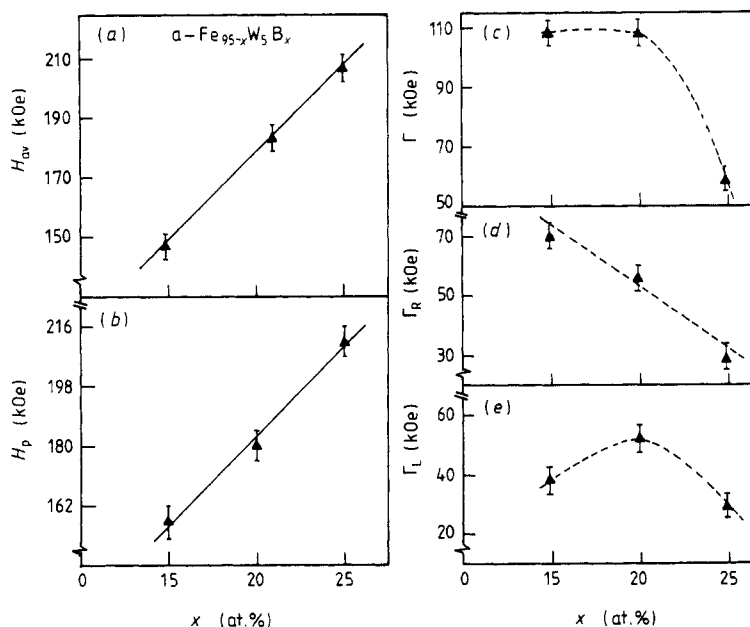


Figure 3. Variations in (a) H_{av} , (b) H_p , (c) Γ , (d) Γ_R and (e) Γ_L with boron concentration for the as-quenched alloys at RT.

width of the most probable magnetic hyperfine field distribution to the left of the most intense field and Γ_R is that to the right of the most intense field. Both H_p and H_{av} appear to increase linearly at rates of 5.4 and 6 kOe (at.%)⁻¹ of boron, respectively. These results appear to be in contradiction to the observed decrease in the saturation magnetisation M_s at 0 K with increasing boron concentration for the present system of alloys (Ramasamy *et al* 1987). Ramasamy *et al* also reported the values of T_c as 399 K, 469 K and 561 K for the $x = 15, 20$ and 25 alloys, respectively. Since T_c for the $x = 15$ composition is close to RT and also since it increases with increasing x , we observe an apparent increase in the values of H_p and H_{av} with x measured at RT. Thus the compositional dependence of saturation magnetic hyperfine field in $Fe_{95-x}W_5B_x$ can be determined only after recording Mössbauer spectra at a substantially lower temperature. This kind of behaviour has also been observed in the case of Fe–B metallic glasses (Chien *et al* 1979, Franke *et al* 1980, Dubois and Le Caer 1982). The presence of boron in the Fe–B amorphous system is responsible for the broadening of most probable magnetic hyperfine field distribution at the low-field wing. The parameters Γ_L and Γ_R represent the B-rich and Fe-rich regions, respectively (Chidambaram Asari 1985). The value of Γ_L is found to increase slightly at first and then to decrease for the $x = 25$ alloy. The values of Γ_R continuously decrease with increasing x .

3.2. Effect of thermal annealing of the alloys on the hyperfine parameters

3.2.1. Isochronal annealing. In the preparation of metallic glasses, because of rapid quenching, the melt deviates from its thermodynamic equilibrium before the temperature reaches the glass transition temperature T_g , and the structure of the glass remains in the high-temperature state. At annealing temperatures $T_a < T_g$, substantial

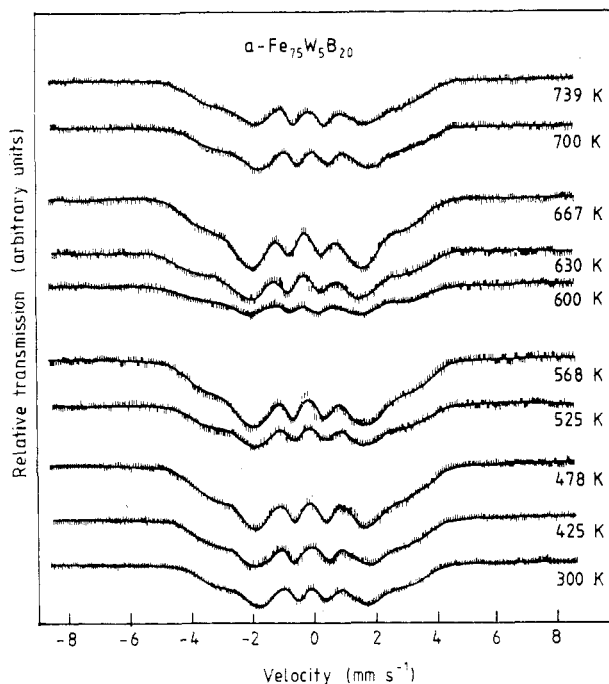


Figure 4. Mössbauer spectra at RT for the isochronally annealed metallic glass for 20 min at the temperatures indicated.

internal atomic rearrangements become experimentally observable as structural relaxation. Annealing induces changes in a large number of physical properties of amorphous alloys (Egami 1978, Chen 1982). Two types of short-range ordering in two different temperature regions of annealing, namely the chemical short-range ordering (CSRO) and topological short-range ordering (TSRO) regions, have been reported for $\text{Fe}_{40}\text{Ni}_{40}\text{B}_{20}$ by van den Beukel *et al* (1986). The present section discusses the effect of isochronal and isothermal annealing on the Mössbauer hyperfine parameters of $\text{Fe}_{95-x}\text{W}_5\text{B}_x$.

Figure 4 shows the Mössbauer spectra of $\text{Fe}_{75}\text{W}_5\text{B}_{20}$ after isochronal annealing for 20 min. Annealing was done at temperatures T_a in the region $T_c < T_a < T_{\text{cr,on}}$ (800 K) where $T_{\text{cr,on}}$ is the onset of crystallisation temperature for the alloy. Similar spectra (not shown in figure 4) were obtained for the $x = 15$ and 25 compositions after annealing in the temperature range between 425 and 700 K for the same duration as for the $x = 20$ alloy. The $x = 15$ and 25 alloys have $T_{\text{cr,on}}$ values of about 725 K and 850 K, respectively, as obtained from the thermomagnetic measurements by Ramasamy *et al* (1987). Figure 5 presents the $P(H)$ distributions obtained by fitting the Mössbauer spectra of isochronally annealed specimens of all three compositions employing the Window method of analysis.

The shape of the $P(H)$ distribution is a representation of the distribution of magnetic moments. The details of the $P(H)$ distribution reflect the nearest-neighbour environment and depend on the coordination number of the Mössbauer probe. In metallic glasses, the varying degrees of distribution in nearest-neighbour distances lead to a distribution of hyperfine magnetic fields. The distribution covers a wide range of magnitudes because of the presence of different nearest-neighbour coordination shells. The observed symmetric $P(H)$ distributions for some annealing temperatures and distorted

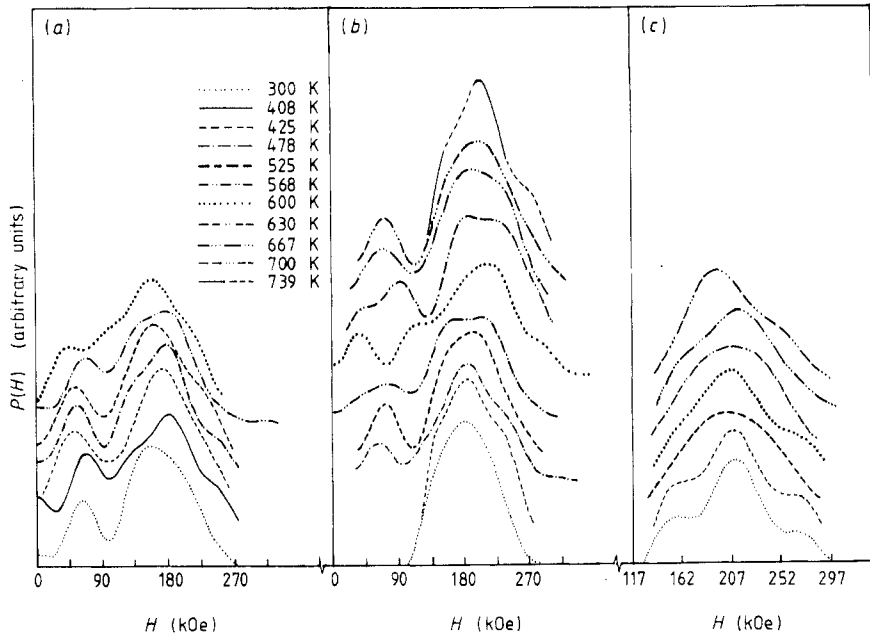


Figure 5. $P(H)$ distribution curves at RT for the $Fe_{95-x}W_5B_x$ metallic glass isochronally annealed for 20 min at the temperatures indicated.

distributions for other annealing temperatures indicate that the environment around the Fe atoms changes with T_a . The low-field peak positions are also found to depend on the temperature of annealing. The low-field peak is absent in all the $P(H)$ spectra obtained for the $x = 25$ alloy. This may be due to the formation of more W–B clusters at the higher B concentration ($x = 25$) as W has a higher affinity towards B than Fe does (Novak *et al* 1982). The formation of W–B clusters will in turn reduce the number of W neighbours of iron and hence the low-field peak disappears.

The values of H_p , H_{av} , Γ_L , Γ_R and Γ obtained from the $P(H)$ distributions are plotted as a function of T_a for the three compositions in figures 6 and 7. It should be noted that the derived values of the parameters Γ_L , Γ_R and Γ are subject to scatter due to variations in the peak shape of the most probable magnetic hyperfine field distribution curves. These variations may be due to the improper parameter values chosen for fitting the Mössbauer spectra by the Window method of evaluation. However, if appropriate values of the parameters are chosen, then the variation in these hyperfine parameters reflects a change in the atomic short-range ordering in the alloy which in turn discloses changes in the structure of amorphous alloys. In figure 6(a), we find that, for the $x = 15$ alloy, H_p initially increases and then falls off with increasing annealing temperature. Annealing at temperatures above 600 K for 20 min leads to crystallisation and hence we limited our measurements to this temperature for the annealing studies. For the $x = 25$ alloy, the trend is reversed as seen in figure 6(c). For the $Fe_{75}W_5B_{20}$ alloy, H_p initially increases (figure 6(b)) up to a T_a of about 560 K and then it falls off sharply at $T_a = 630$ K by about 18% of the value for the as-quenched state. Thereafter it again shows an increase. The most probable hyperfine magnetic field corresponds to the most probable configuration of the Fe nearest-neighbour distributions in the alloy and is sensitive to

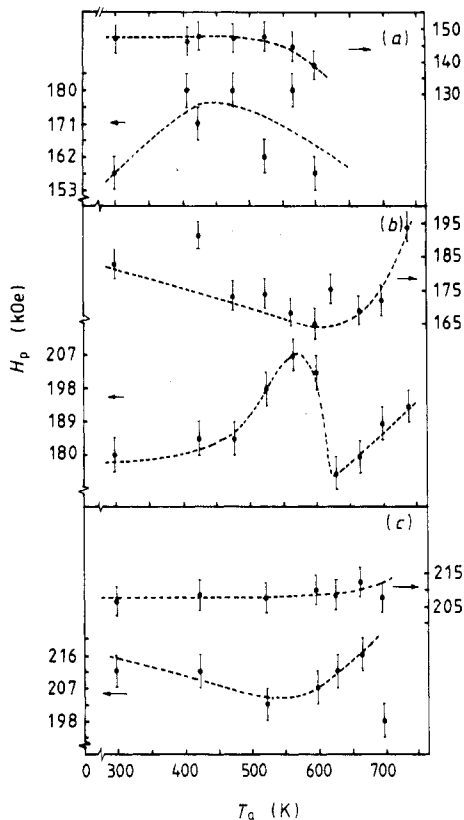


Figure 6. Variations in H_p (○) and H_{av} (●) with annealing temperature T_a for the (a) $x = 15$, (b) $x = 20$ and (c) $x = 25$ alloys (annealing time $t_a = 20$ min).

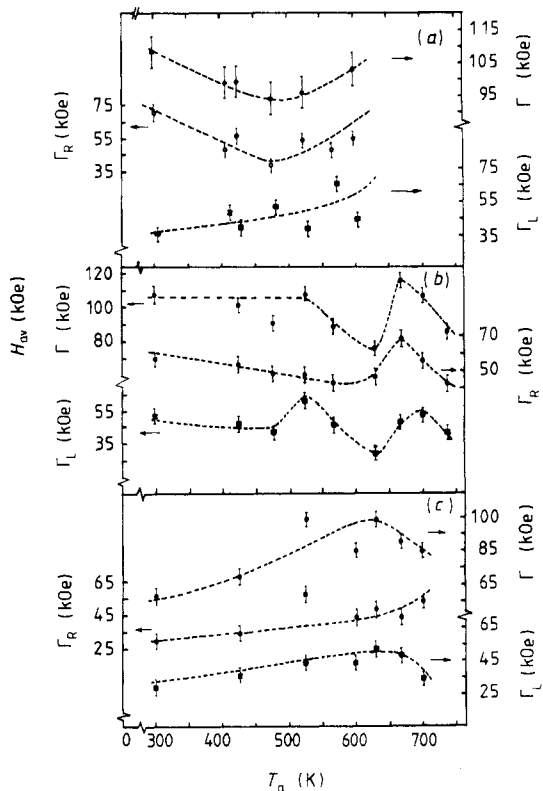


Figure 7. Variations in Γ_L (■), Γ_R (○) and Γ (●) as functions of annealing temperature T_a for the (a) $x = 15$, (b) $x = 20$ and (c) $x = 25$ alloys ($t_a = 20$ min).

changes in CSRO (Kemeny *et al* 1980). Changes in H_p , H_{av} , etc, with the thermal annealing can be associated with changes in atomic short-range ordering (Chidambaram Asari 1985). Variations in the Mössbauer parameters with T_a can also be discussed by analogy with the results of MAE studies (Bahgat *et al* 1986). The MAE studies deal with changes in the structural and magnetic stabilities of the amorphous alloys with the magnetic field applied for a fixed duration of time. We compare our results with those obtained from the MAE spectra by Kiss *et al* (1984) for the $\text{Fe}_{75}\text{W}_5\text{B}_{20}$ alloy. In the present study, H_p reaches a maximum when T_a is 560 K. Similarly Kiss *et al* also observe a maximum in the MAE for the $\text{Fe}_{74.6}\text{W}_{5.4}\text{B}_{20}$ metallic glass, at a value of approximately 468 K for T_a . These maxima are attributed to the relaxation of boron atoms via transitions between 'anomalous interstitial sites' (Kronmüller and Moser 1982). The difference in the temperatures at which these maxima occur may be due to the different annealing conditions in the two studies. In general, the variations in H_p with annealing temperatures may be correlated with the rearrangement of boron atoms due to relaxation for all the three compositions.

Any change in free volume would affect all the atomic configurations of nearest-neighbour distributions in the alloy and hence one could expect variations in H_{av} due to

changes in TSRO (Allia *et al* 1982, Chidambaram Asari 1985). Figure 6 shows variations in H_{av} with annealing for the present system. As in the case of the H_p variation, we observe an opposite trend in the variation in H_{av} at higher annealing temperatures for the $x = 15$ and 25 alloys. At lower T_a -values (less than 525 K), H_{av} remains almost constant for the above two alloys. For the alloy with $x = 20$, an increase is found for $T_a > 600$ K as in the case of the $x = 25$ alloy. These results show that only at high annealing temperatures does structural relaxation arise from TSRO in addition to the contributions from CSRO. These results are also supported by the changes in T_c observed for the present system by Ramasamy *et al* (1987). However, in the region $T_a < 600$ K, H_{av} decreases for the $x = 20$ alloy. The cause for this behaviour is not at present understood.

The variation in the left half-width Γ_L of the most probable field distribution with T_a for all the three compositions is shown in figure 7. An initial increase in Γ_L is observed for the $x = 15$ and 25 alloys at low temperatures. As in the case of H_p and H_{av} variations, there is again an opposite trend in the variation in Γ_L at higher annealing temperatures for these two compositions. The variation in Γ_L can be related to the mobility of boron atoms towards a state of thermodynamical equilibrium of the alloy (Chidambaram Asari 1985). The $x = 20$ alloy exhibits a behaviour different from that for the $x = 15$ and 25 alloys. It can also be noticed that the variations in H_p and Γ_L for the $x = 20$ alloy are more or less similar. This shows that the variations are due to CSRO which is mainly due to the rearrangement of boron atoms. Variation in the right half-width Γ_R of the most probable distribution with T_a for the present system is shown in figure 7. These variations are found to be different for each of the alloys. The values of Γ_R give a picture of the Fe-rich environments. A decrease in the value of Γ_R can be attributed to an increase in the number of Fe-B pairs in these alloys (Chidambaram Asari 1985).

Figure 7 shows the variation in the FWHM Γ of the most probable distribution of hyperfine field. The FWHM is an important parameter as it is a measure of the distribution of atomic short-range ordering. Γ is found to vary in opposite directions for the $x = 15$ and 25 compositions not only for higher annealing temperatures (as in the case of H_p , H_{av} and Γ_L) but also for lower T_a -values. Both Γ_L and Γ for the $x = 20$ alloy vary in a similar manner. This indicates the dominant role of Γ_L , which is due to the rearrangement of boron atoms with annealing. One also notices that the $x = 25$ alloy has comparatively smaller values for Γ which means a higher degree of atomic short-range ordering for this composition. Kemeny *et al* (1980) observe a broader distribution of $P(H)$ for the $(Fe_{33}Ni_{67})_{75}B_{25}$ metallic glass than that for the $(Fe_{25}Ni_{75})_{80}B_{20}$ metallic glass. They obtained these distributions at 5 K in the as-received state. For both the alloys, they also determined changes in T_c (i.e. ΔT_c) due to isochronal annealing at $T_a < T_{cr}$, where T_{cr} is the crystallisation temperature of the alloy. Since the width of the $P(H)$ distribution is narrower and ΔT_c is smaller for the $(Fe_{25}Ni_{75})_{80}B_{20}$ alloy, they conclude that the atomic ordering might be relatively high for this alloy in the as-received state itself and only very small changes in the CSRO could be expected on thermal annealing. A similar observation has been made in the present system. The alloy $Fe_{70}W_5B_{25}$ has a smaller value of Γ at RT than at the other two compositions and gives rise to a value of about 4.4 K for ΔT_c when isochronally annealed at 698 K, i.e. below its T_{cr} (Ramasamy *et al* 1987), whereas a similar annealing treatment for the $x = 15$ and 20 alloys, which have larger values of Γ at RT than that of the $x = 25$ alloy, yielded higher values of ΔT_c , namely 10 and 7.3 K. Thus, we find that our observations are in agreement with those of Kemeny *et al*.

The opposite trends in the variation in Mössbauer parameters observed for the $x = 15$ and $x = 25$ alloys at higher T_a -values are analogous to those obtained by Luborsky

and Liebermann (1978) for the Fe–B system. They have observed that the density, stress relaxation and activation energy for crystallisation change with boron content. They find that a plot of each of these quantities versus boron content comprises two linear regions of different slopes with the transition in slope occurring at about 20–21 at. % B which is in the eutectic region. They state these changes in slope can be related to changes in the dense random packing (DRP) structure of the system. According to the model of the (DRP) of hard spheres, the Bernal holes (Luborsky and Liebermann 1978) can accommodate up to 21 at. % of suitably smaller metalloid atoms (i.e. boron). When the boron content is less than 21 at. %, there will be an excess of large Bernal holes. In such alloys, relaxation takes place through diffusion by a mechanism analogous to that found in crystalline alloys with excess vacancies. However, when the boron content is greater than 21 at. %, relaxation may take place through the migration of metalloid atoms by a mechanism of self-diffusion which is independent of boron concentration. In the present system also, Nielsen (1980) reports the density values at RT for the $x = 15, 20$ and 25 alloys as 8.34 g cm^{-3} , 8.38 g cm^{-3} and 8.16 g cm^{-3} , respectively, i.e. the density is maximum for 20 at. % B and decreases on both sides of this concentration. Similarly, we have observed that the Mössbauer parameters, namely H_p , H_{av} , Γ_L , Γ_R and Γ , which are sensitive to structural relaxation show an opposite trend of variation on either side of the 20 at. % B concentration. Following Luborsky and Liebermann, we could also very well attribute the present results to a change in the DRP structure of the Fe–W–B system at 20 at. % B concentration.

3.2.2. Isothermal annealing. The effect of isothermal annealing on one of the above alloys namely the Fe₇₅W₅B₂₀ metallic glass, is discussed in the present section. The alloy was annealed at 478 K which is just above its T_c (469 K) since we expect a significant internal atomic rearrangement at temperatures $T_c < T_a < T_{cr}$. RT Mössbauer spectra were recorded after each successive annealing of the alloy at 478 K for 10 min up to a total of 60 min. The $P(H)$ distributions obtained are shown in figure 8(A). One observes the appearance and disappearance of the low-field peak with annealing time t_a . No structure is markedly seen in $P(H)$ distributions unlike in the case of isochronally annealed specimens. Figure 8(B) depicts the observed changes ΔH_p , $\Delta \Gamma_L$ and $\Delta \Gamma$ in the Mössbauer parameters with the time of annealing. One can see that $\Delta \Gamma$ remains almost invariant, indicating that the distribution of Fe moments in the alloy does not change with t_a . The increase in ΔH_p with annealing time t_a shows the progress of CSRO with t_a , and the increase in $\Delta \Gamma_L$ indicates that the CSRO is due to the rearrangement of boron atoms. These results support those observed for the change in T_c with t_a for the same system (Ramasamy *et al* 1987).

3.3. Crystallisation studies

Metallic glasses crystallise by the nucleation and growth process which is controlled by the interfacial energy between amorphous and crystalline phases and by diffusivity. Therefore, it is a kinetic process dependent on both temperature and time. The kinetics of the crystallisation process depends on a variety of parameters such as the mode of crystallisation, the number of quenched-in nuclei, the activation energy for diffusion and finally the driving force, i.e. the difference between the free energy of the amorphous and those of possible crystalline phases. Crystallisation studies of Fe–B metallic glass systems have been made by many researchers (Franke *et al* 1978, Luborsky and Liebermann 1978, Greer 1982, Alp *et al* 1984). There are reports in the literature on

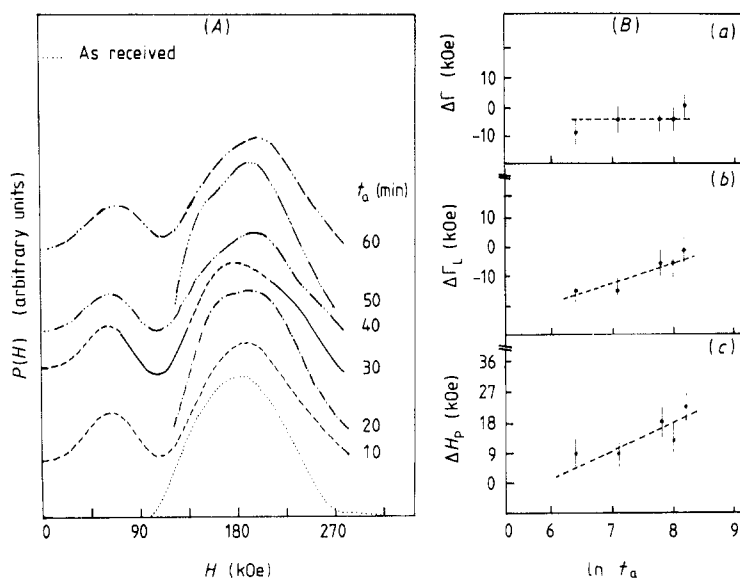


Figure 8. (A) $P(H)$ distribution curves and (B) variations in (a) $\Delta\Gamma$, (b) $\Delta\Gamma_L$ and (c) ΔH_p at RT for the isothermally annealed $Fe_{75}W_5B_{20}$ metallic glass at 478 K for the durations indicated.

crystallisation and thermal stability studies of ternary Fe–TM–B alloys (Köster and Herold 1981, Battezzati *et al* 1987). Ternary alloys are found to be more stable against crystallisation than are the binary systems. Battezzati *et al* (1987) report that alloys of the type Fe–TM–B (TM \equiv Ti, V, Cr, Mn, Co, Ni and Cu) show a high resistance to crystallisation. Leake and Rout (1988) state that, when the added TM is one of the elements to the left of Fe in the periodic table, the alloy exhibits an increase in $T_{cr,on}$ (or thermal stability), the increase being greater when the element is farther from Fe.

From the thermomagnetic curves of the present alloys (Ramasamy *et al* 1987), we find that the onset of crystallisation of the alloys takes place at about 700 K, 725 K and 800 K, for the $x = 15, 20$ and 25 alloys and the alloys become fully crystallised at about 1070 K. The $x = 25$ alloy, which has the highest thermal stability in the present system of alloys, was annealed at 1073 ± 5 K for an hour and the Mössbauer spectrum recorded at RT is shown in figure 9(b). The experimental spectrum has been computer fitted using the least-squares method developed by Bent *et al* (1969). The spectrum shows a complex profile, indicating the presence of many crystalline phases. For this spectrum, we found that with an arbitrary ratio of spectral linewidths, namely 1.0:0.9:0.8:0.8:0.9:1.0 for all the six-line patterns yielded a better fit than without such a correction. The full curve is the result of such a fitting. The spectrum consists of five sextets plus a non-magnetic doublet. These component spectra are individually indicated by the bar diagrams. The relative intensities of the Mössbauer lines are given by the heights of the bars. The hyperfine magnetic fields, the various crystalline phases identified and their relative intensities are given in table 1. Our x-ray diffraction results (Ramasamy *et al* 1987) show the presence of the α -Fe, $(Fe_{0.8}W_{0.2})_3B$, Fe_2B and $FeWB$ crystalline phases and also an unidentified phase for the $Fe_{70}W_5B_{25}$ metallic glass annealed at 1073 K. From the Mössbauer parameters of the crystallised $Fe_{70}W_5B_{25}$ metallic glass given in table 1, it is clear that set I arises from the α -Fe phase. Both the x-ray diffraction and the magnetisation studies (Ramasamy *et al* 1987) confirm the presence of this phase. The $Fe_3B(t)$

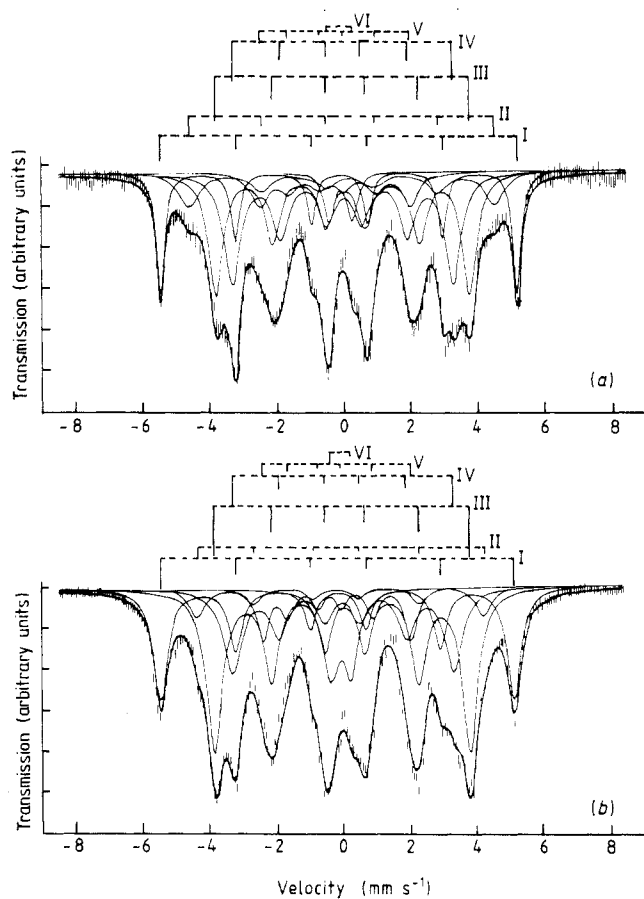


Figure 9. RT Mössbauer spectra for the (a) $x = 20$ and (b) $x = 25$ alloys crystallised at 1073 K for 1 h.

phase has three distinct Fe sites and the corresponding Mössbauer spectra have hyperfine magnetic fields as 300, 275 and 230 kOe at RT (Sausegua and Morrish 1982, Franke *et al* 1978). The Mössbauer spectra marked as sets II and IV in table 1 can be ascribed to the $(\text{Fe}_{0.8}\text{W}_{0.2})_3\text{B}$ phase as confirmed by the x-ray diffraction studies (Ramasamy *et al* 1987). The lower values of the observed hyperfine magnetic fields are due to the substitution of W for Fe in the Fe_3B phase. The observation of only two sextets for this phase may be due to the selective substitution of W in one of the three crystalline sites as suggested by Klein *et al* (1982). Also, the high value of the FWHM (0.65 mm s^{-1}) for set IV does not rule out the possibility of the overlapping of the two low-field sextets of the $(\text{Fe}, \text{W})_3\text{B}$ phase.

The Mössbauer sextet denoted as set III can be unambiguously assigned to the Fe_2B phase as its Mössbauer parameters agree very well with those of crystalline Fe_2B . The notion that W does not enter into this phase is supported by both the Mössbauer parameters and the T_c -value determined from the magnetisation studies (Ramasamy *et al* 1987). Set V can be assigned to an unidentified phase as also seen in the x-ray studies. This phase is not seen in the thermomagnetic studies (Ramasamy *et al* 1987), which may

Table 1. Mössbauer hyperfine parameters of the Fe–W–B metallic glass system crystallised by thermal annealing and the identified crystalline phases.

Metallic glass	Annealing temperature (K)	Annealing time (h)	Set No.	H_{hf} (kOe)	Relative intensity (%)	Phases identified
$Fe_{70}W_5B_{25}$	1073	1	I	327.7	21.2	α -Fe
			II	265.7	5.9	$(Fe_{0.8}W_{0.2})_3B$
			III	236.9	35.2	Fe_2B
			IV	205.3	20.3	$(Fe_{0.8}W_{0.2})_3B$
			V	137.8	8.2	^a
			VI	—	9.3	$FeWB^b$
$Fe_{75}W_5B_{20}$	1073	1	I	329.8	16.8	α -Fe
			II	282.0	11.3	$(Fe, W)_3B$
			III	234.2	29.5	Fe_2B
			IV	203.7	29.2	$(Fe, W)_3B$
			V	140.0	9.2	^a
			VI	—	4.0	$FeWB^b$
$Fe_{80}W_5B_{15}$	739	$\frac{1}{3}$	I	330.9	13.1	α -Fe
			II	293.0	18.3	$(Fe, W)_3B$
			III	225.0	23.8	Fe_2B
			IV	171.0	13.8	$(Fe, W)_3B$
			V	127.0	18.4	^a
			VI	—	12.6	$FeWB^b$
$Fe_{80}W_5B_{15}$	1073	1	I	332.4	16.9	α -Fe
			II	280.0	15.9	$(Fe, W)_3B$
			III	231.1	35.1	Fe_2B
			IV	203.7	20.0	$(Fe, W)_3B$
			V	142.0	7.4	^a
			VI	—	4.6	$FeWB^b$

^a Unidentified.^b Non-magnetic.

be due to a relatively small intensity of this phase. The non-magnetic phase denoted as set VI on the Mössbauer spectrum can be taken to be $FeWB$ phase as observed in the x-ray studies. Because of its large W content, it is possible that the $FeWB$ phase is non-magnetic. Thus, in the light of the above discussions, one concludes by correlating the results of Mössbauer, x-ray diffraction and thermomagnetic studies that the crystalline phases obtained on thermally annealing the $Fe_{70}W_5B_{25}$ metallic glass at 1073 K for an hour are α -Fe, Fe_2B , $(Fe_{0.8}W_{0.2})_3B$, $FeWB$ and an unidentified phase.

The Mössbauer spectrum of the $x = 20$ alloy (figure 9(a)) annealed in the same way also shows the presence of all the above phases but with slightly different relative intensities due to the difference in the boron concentration. As evident from the thermomagnetic curves (Ramasamy *et al* 1987), the relative amounts of Fe and W in the $(Fe, W)_3B$ phase may be different when compared with that in the $x = 25$ alloy.

As shown in table 1, the same crystalline phases have been observed for the $x = 15$ alloy annealed under conditions identical with those of the other two compositions. The corresponding fitted spectrum is shown in figure 10(b). The interesting result is that all the phases observed for 1073 K annealing are also present even for a lower temperature

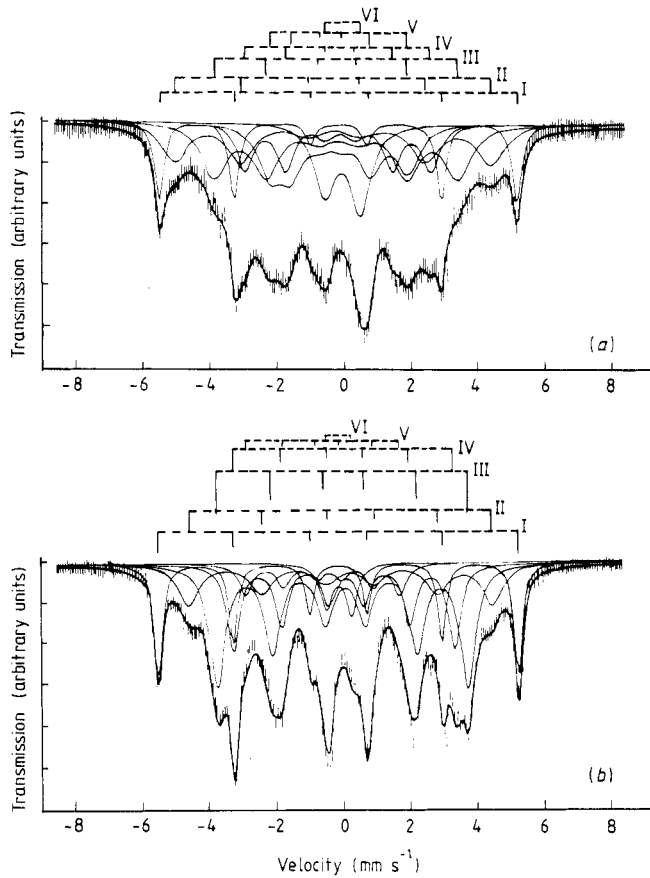


Figure 10. RT Mössbauer spectra for the $\text{Fe}_{80}\text{W}_5\text{B}_{15}$ alloy crystallised at (a) 739 K for 20 min and (b) 1073 K for 1 h.

of annealing, i.e. at 739 K, which is close to its $T_{\text{cr,on}}$ (725 K) (figure 10(a)). The simultaneous precipitation of all the crystalline phases when annealed at temperatures close to the value of $T_{\text{cr,on}}$ is a characteristic of the eutectic type of reaction (Köster and Herold 1981). By looking at table 1, we find that the α -Fe phase has increased in relative intensity from 13.1% at 739 K to 16.9% at 1073 K and also that of the Fe_2B phase has increased from 23.8 to 35.1%. The simultaneous increases in the relative intensities of α -Fe and Fe_2B phases are also an indication of the eutectic type of crystallisation (Cusido *et al* 1985) in the present alloy. This observation for the $\text{Fe}_{80}\text{W}_5\text{B}_{15}$ metallic glass supports the earlier results of Zemcik *et al* (1987) for the Fe–V–B system and those of Köster and Herold (1981) for the Fe–Mo–B and Fe–Co–B metallic glasses.

4. Conclusions

The results of the Mössbauer effect studies made on the $\text{Fe}_{95-x}\text{W}_5\text{B}_x$ metallic glass system may be summarised as follows.

(i) The model-independent continuous field distribution method of Window is found to be appropriate and yields reliable $P(H)$ distributions for the metallic glasses when the number of cosine terms in the Fourier series is between 12 and 15.

(ii) The RT values of the most probable hyperfine magnetic field H_p and the average hyperfine field H_{av} show an apparent and linear increase with boron concentration in the as-quenched state. For the $x = 25$ alloy, the structure in the $P(H)$ distribution indicates three different local environments for Fe atoms.

(iii) The variation in the Mössbauer hyperfine parameters with thermal annealing for all the three compositions implies the existence of structural relaxation due to CSRO at low annealing temperatures and also due to TSRO at higher annealing temperatures. The opposite trend observed in the variation in the hyperfine parameters at high annealing temperatures for the $x = 15$ and 25 alloys may be due to changes taking place in the DRP structure of the system with 20 at. % boron concentration.

(iv) The Mössbauer spectra of the crystallised $Fe_{80}W_5B_{15}$ alloy show that the alloy undergoes a eutectic type of crystallisation. The crystalline phases identified in the Fe–W–B system are α -Fe, Fe_2B , $(Fe_{0.8}W_{0.2})_3B$ and non-magnetic FeWB.

Acknowledgments

The authors are grateful to Dr H J V Nielsen and Dr O V Nielsen, Department of Electrophysics, Technical University of Denmark, Lyngby, for kindly providing the metallic glass ribbons for the present study. One of us (KG) would like to thank the University Grants Commission (UGC) for having offered him the Research Fellowship during the course of this work. The facilities available under the UGC-COSIST program are also acknowledged.

References

- Allia P, Ferro Milone A, Vinai F, Fratucello G and Ronconi F 1982 *J. Appl. Phys.* **53** 7750
 Alp E E, Simon K M, Saporoschenko M and Brower W E Jr 1984 *J. Non-Cryst. Solids* **61–2** 871
 Bahgat A A, Shaisha E E and El-Kottamy M H 1986 *J. Mater. Sci. Lett.* **5** 864
 Battezzatti L, Antonione C and Riontino G 1987 *J. Non-Cryst. Solids* **89** 114
 Bent M F, Persson B and Agresti D G 1969 *Comput. Phys. Commun.* **1** 67
 Bhatnagar A K and Bhanu Prasad B 1985 *J. Appl. Phys.* **57** 3514
 Chen H S 1982 *Phys. Scr.* **25** 726
 Chidambaram Asari U 1985 *PhD Thesis* University of Madras, India
 Chien C L and Hasegawa R 1978 *J. Appl. Phys.* **49** 1721
 Chien C L, Musser D, Gyorgy E M, Sherwood R C, Chen H S, Luborsky F E and Walter J L 1979 *Phys. Rev.* **B 20** 283
 Cusido J A, Isalgue A and Tejada J 1985 *Phys. Status Solidi a* **87** 169
 Dubois J M and Le Caer G 1982 *Nucl. Instrum. Methods* **199** 307
 Egami T 1978 *Mater. Res. Bull.* **13** 557
 Franke H, Dey S, Rosenberg M, Luborsky F E and Walter J L 1980 *J. Magn. Magn. Mater.* **15–8** 1364
 Franke H, Herold U, Köster U and Rosenberg M 1978 *J. Magn. Magn. Mater.* **9** 214
 Ganesan K, Narayanasamy A and Nagarajan T 1988 *Proc. Sol. State. Phys. Symp. (India)* **31C** 237
 Gopinathan K P, Sundar C S, Bharathi A, Narayanasamy A and Chidambaram Asari U 1982 *Proc. Int. Conf. on Applications of the Mössbauer Effect (Jaipur)* (New Delhi: Indian National Science Academy) p 350
 Granasy L, Lovas A, Kiss L, Kemeny T and Kisdi-Koszo E 1982 *J. Magn. Magn. Mater.* **26** 109
 Greer A L 1982 *Acta Metall.* **30** 171
 Kemeny T, Schaffsma A S, Donald I W, Davies H A, Fogarassy B, Vincze I and van den Woude 1980 *J. Physique Coll.* **41 C8** 878

- Kisdi-Koszo E, Lovas A, Vojtanik P, Boskovicova M and Potocky L 1982 *J. Magn. Magn. Mater.* **26** 121
- Kiss L F, Ashry A, Toth F I and Zambo-Balla K 1984 *J. Magn. Magn. Mater.* **41** 391
- Klein H P, Ghafari M, Ackermann M, Gonser U and Wagner H G 1982 *Nucl. Instrum. Methods* **199** 159
- Konczos Z, Kisdi-Koszo E, Lovas A, Kajsos Zs, Potocky L, Daniel-Szabo J, Kovac J and Novak L 1984 *J. Magn. Magn. Mater.* **41** 122
- Köster U and Herold U 1981 *Glassy Metals I (Topics in Applied Physics 46)* ed H J Guntherodt and H Beck (Berlin: Springer) p 225
- Kronmüller H and Moser N 1982 *Amorphous Magnetic Alloys* ed F E Luborsky (London: Butterworths) section 16
- Leake J A and Rout J E 1988 *Mater. Sci. Eng.* **97** 325
- Lin S T, Jang L Y, Ku W T, Chou L S and Yao Y D 1981 *Proc. 4th Int. Conf. on Rapidly Quenched Metals*, ed T Masumoto and K Suzuki (Sendai: Japan Institute of Metals) p 1105
- Lovas A, Potocky L, Novak L, Kisdi-Koszo E and Zambo-Balla K 1980 *Central Research Institute for Physics, Hungary, Report KFKI-94*
- Luborsky F E and Liebermann H H 1978 *Appl. Phys. Lett.* **33** 233
- Narayanasamy A, Nagarajan T, Muthukumarasamy P and Radhakrishnan T S 1979 *J. Phys. F: Met. Phys.* **9** 2261
- Nielsen H J V 1980 *Phys. Status Solidi a* **61** K111
- Novak L, Potocky L, Uliciansky S, Kisdi-Koszo E, Lovas A, Takacs J and Mlynek R 1982 *Nucl. Instrum. Methods* **199** 118
- Ramasamy S, Lundgren L, Ganesan K and Narayanasamy A 1987 *J. Phys. F: Met. Phys.* **17** 753
- Sas B, Kemeny T and Toth J 1986 *Solid State Commun.* **59** 195
- Sausegua N and Morrish A H 1982 *Phys. Rev. B* **26** 305
- Takacs L, Konczos G, Zambo-Balla K and Vertes A 1984 *J. Magn. Magn. Mater.* **41** 110
- Toth J, Sas B and Konczos G 1985 *Proc. 5th Int. Conf. On Rapidly Quenched Metals* ed S Steeb and H Warlimont (Amsterdam: Elsevier) p 1071
- van den Beukel A, Huizer E, Mulder A L and van der Zwaag S 1986 *Acta Metall.* **34** 483
- Window B 1971 *J. Phys. E: Sci. Instrum.* **4** 401
- Zemcik T, Jakesova M and Jiraskova Y 1987 *Czech. J. Phys. B* **37** 24